J. Fluid Mech. (1968), *vol.* 34, *part* 2, *pp.* 273–297
Printed in Great Britain

Stability of towed, totally submerged flexible cylinders

By M. P. PAIDOUSSIS

Department of Mechanical Engineering, McGill University, Montreal

(Received 5 February 1968)

A general theory is presented to account for the small, free, lateral motions of a flexible, slender, cylindrical body with tapered ends, totally submerged in liquid and towed at steady speed U. For particular shapes of the ends and length of tow-rope, it is shown that the body may be subject to oscillatory and non-oscillatory instabilities for $U > 0$; at small U, these instabilities correspond to those of a rigid body. At higher U, the system generally regains stability in the above modes, but may be subject to higher-mode, flexural oscillatory instabilities. The critical conditions of stability are calculated extensively and the effect on stability of a number of dimensionless parameters is discussed. It is shown that optimum stability is achieved with a streamlined nose, a blunt tail and a short tow-rope.

Some experiments are described which were designed to test the theory. Rubber cylinders of neutral buoyancy were held in vertical water flow by a nylon 'tow-rope'. Provided the tail was streamlined and the tow-rope not too short, 'criss-crossing', non-flexural oscillations developed at very low flow. Increasing the flow, these oscillations ceased and the cylinder buckled like a column; subsequently higher-mode flexural oscillations developed. However, for a sufficiently blunt tail and short tow-rope, the system was completely stable.

The experimental observations are generally in qualitative agreement with theory. Quantitative comparison of the various instability thresholds and stable zones between experiment and theory, based on estimated values of some of the theoretical dimensionless parameters, is also fairly good.

1. Introduction

This study deals with the dynamics of submerged flexible slender cylinders held in axial flow by a string attached to the upstream end; the system thus simulates a flexible cylinder towed underwater.

This work is an extension of a previous study of the dynamics of flexible cylinders in axial flow (Paidoussis 1966*a*, *b*), in which the upstream end of the cylinder, or both ends, were supported. In this previous study it was found that for sufficiently large flow velocities the cylinder may be subject to buckling and oscillatory instabilities in its first and higher flexural modes, respectively. The buckling instability is similar to the buckling of a column under static loading; the oscillatory instabilities are self-excited oscillations similar to flutter. It was considered likely that the system under consideration here, namely that of a towed cylinder, may be subject to similar instabilities.

This problem was first examined by Hawthorne (1961) in connexion with the observed 'snaking' of towed Dracones, which are flexible, sausage-like towed barges, used for the transport of fluid cargo. In his analysis, Hawthorne dealt exclusively with the buckling mode of instability; he found that the critical towing speeds for buckling agreed fairly closely with the observed speeds for the onset of snaking. The analysis presented here is considerably more general.

The problem at hand is of course related to that of stability of towed ships, and that of yawing of airships moored to a mast. Wherever possible, the results obtained will be compared to those from the above related theories.

2. General theory

Equation of small motions

The system under study consists of a flexible slender cylindrical body of circular cross-section immersed in an incompressible fluid of density ρ flowing with uniform velocity U parallel to the x-axis, which coincides with the position of

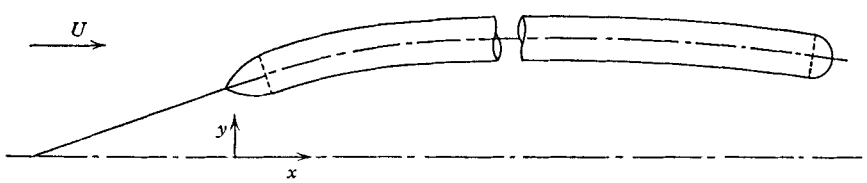

FIGURE 1. Diagram of a towed slender flexible cylinder.

rest of the cylinder and of the tow-rope. At its extremities the cylinder is terminated by ogival or hemispherical ends (figure 1) which are short in comparison with the over-all length of the body, L. Apart from these end-sections, the cylinder is of uniform cross-sectional area S, mass per unit length m and flexural rigidity EI. The tow-rope is considered to be inextensible and of negligible rigidity and mass.

The specific gravity of the cylinder is supposed to be equal to that of the flowing fluid. The x- and y-axes lie in a horizontal plane wherein all motions of the cylinder are supposed to be confined, so that gravity and buoyancy do not come into play. (The question of applicability of this theory to the general case of a towed cylinder equally free to move in any plane is discussed in §7.)

The equation of small lateral motions for such a cylindrical body about its position of rest was derived previously (Paidoussis 1966*a*) and, consequently, a complete derivation will not be given here.

Consider an element δx of the cylinder (figure 2) which was subjected to a small lateral motion $y(x,t)$. We denote the axial tension by T, the lateral force per unit length due to acceleration of the fluid around the cylinder by F_A, and the viscous forces per unit length in the normal and longitudinal directions by F_N and F_L, respectively. A force balance in the lateral direction yields

$$EI\frac{\partial^4 y}{\partial x^4}+F_A-\frac{\partial}{\partial x}\left(T\frac{\partial y}{\partial x}\right)+F_N+m\frac{\partial^2 y}{\partial t^2}=0, \tag{1}$$

where the first term was obtained, by elementary beam theory, by relating the lateral shear force Q to the bending moment $\mathscr{M}$.

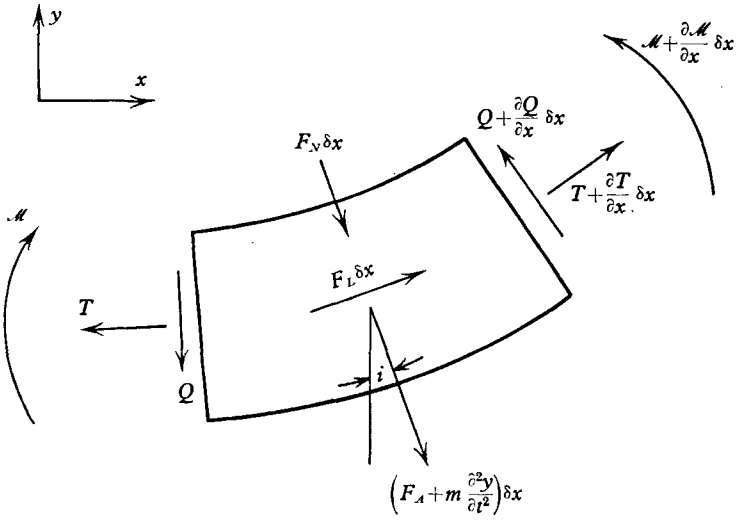

FIGURE 2. Forces and moments acting on an element δx of the cylinder.

The force $F_A\,\delta x$ represents the reaction on the cylinder of the force required to accelerate the fluid around it, and may be written as

$$F_A\,\delta x = [(\partial/\partial t) + U(\partial/\partial x)]\,(Mv)\,\delta x$$

(Lighthill 1960). The relative velocity $v(x,t)$ between the cylinder and the fluid flowing past it, resulting from motion of the cylinder, is given by

$$v(x,t) = [(\partial/\partial t) + U(\partial/\partial x)]y;$$

M is the virtual mass of the fluid per unit length (equal to ρS for a circular cylinder). Hence we may write

$$F_A = M\left(\frac{\partial}{\partial t} + U\frac{\partial}{\partial x}\right)^2 y \tag{2}$$

over the cylindrical portion of the body, where $M = \rho S$ is constant. (The forces acting on the tapered portions of the body will be treated with the boundary conditions.)

The viscous forces acting on long inclined cylinders have been discussed by Taylor (1952). For turbulent boundary layers Taylor noted that viscous forces will depend on the exact nature of surface roughness. Where it may be assumed that roughness consists of a number of projections pointing equally in all directions, he proposed that

$$F_N = \tfrac{1}{2}\rho DU^2(C_{Dp}\sin^2 i + C_f \sin i) \quad \text{and} \quad F_L = \tfrac{1}{2}\rho DU^2 C_f \cos i,$$

where i is the angle of incidence, D is the cylinder diameter, and C_{Dp} and C_f are the coefficients associated with form and friction drag for a cylinder in cross flow.

For the motions considered here $\sin i \ll 1$ and, as only linear terms will be

considered in the analysis, it is assumed that the viscous forces may be represented adequately by

$$F_N = \tfrac{1}{2}(M/D)\,U^2 c_N \sin i \quad \text{and} \quad F_L = \tfrac{1}{2}(M/D)\,U^2 c_T,$$

in which ρ was eliminated by the use of $M = \frac{1}{4}\pi D^2 \rho$; c_N and c_T are considered to be not necessarily equal. The angle i may be related to the normal and axial components of flow by $i = \sin^{-1}(v/U)$, which substituted in the above equation along with the expression for v given above yields

$$F_N = \tfrac{1}{2} c_N \frac{M}{D} U \left(\frac{\partial y}{\partial t} + U \frac{\partial y}{\partial x}\right) \quad \text{and} \quad F_L = \tfrac{1}{2} c_T \frac{M}{D} U^2. \tag{3}$$

For small lateral motions, inertial forces in the axial direction may be neglected; accordingly, an axial force balance on the element δx yields $\partial T/\partial x + F_L = 0$. Substituting from (3), integration from x to $x = L$ yields

$$T(x) = T(L) + \tfrac{1}{2} c_T M U^2 (L - x)/D.$$

A non-zero value of $T(L)$ can only arise from form drag at the free end, which may be considered proportional to $\frac{1}{2}\rho U^2 S$. Accordingly, we write

$$T(x) = \tfrac{1}{2} c_T M U^2 (L - x)/D + \tfrac{1}{2} c_2 M U^2, \tag{4}$$

where c_2 is the coefficient of form drag at the tail.

Substituting now (2), (3) and (4) into (1), we obtain the equation of small lateral motions

$$EI \frac{\partial^4 y}{\partial x^4} + M \left(\frac{\partial}{\partial t} + U \frac{\partial}{\partial x}\right)^2 y - \frac{\partial}{\partial x}\left\{\left[\tfrac{1}{2} c_T \frac{(L-x)}{D} + \tfrac{1}{2} c_2\right] M U^2 \frac{\partial y}{\partial x}\right\} + \tfrac{1}{2} c_N \frac{MU}{D}\left(\frac{\partial y}{\partial t} + U \frac{\partial y}{\partial x}\right) + m \frac{\partial^2 y}{\partial t^2} = 0. \tag{5}$$

If distributed longitudinal drag is neglected ($c_T = 0$), this equation reduces to essentially that derived by Hawthorne (1961).

Boundary conditions

At either end, it is assumed that the cross-sectional area tapers smoothly from S to zero in a distance sufficiently short, so that y and the lateral velocity v may be considered constant. This requirement allows the forces acting at the tapered ends to be lumped and considered in appropriate boundary conditions (Hawthorne 1961; Paidoussis 1966*a*). Equating the lateral shear and inertial forces to the rate of change of lateral momentum over the tapered free end, say for $L - l_2 < x < L$, we obtain

$$\int_{L-l_2}^{L} \frac{\partial Q}{\partial x}\,dx - f_2 \int_{L-l_2}^{L} \left(\frac{\partial}{\partial t} + U \frac{\partial}{\partial x}\right)[M(x)\,v(x,t)]\,dx - \int_{L-l_2}^{L} m(x) \frac{\partial^2 y}{\partial t^2}\,dx = 0, \tag{6}$$

where Q is the lateral shear force. The parameter f_2, which is equal to unity for slender-body, inviscid flow theory, was introduced to account for the theoretical lateral force at the free end not being fully realized because of (*a*) the lateral flow not being truly two-dimensional, since the fluid has opportunity to pass around rather than over the tapered end (Munk 1924), and (*b*) boundary-layer effects (Hawthorne 1961). Accordingly, f_2 will normally be less than unity.

At the upstream end, there is also a tow-rope force, equal to the tow-rope tension, P, times the sine of the angle that the tow-rope makes with the position of rest. For small motions this is linearized to $-P(y/s)$, where s is the tow-rope length. Accordingly, at the upstream end we have

$$\int_0^{l_1} \frac{\partial Q}{\partial x}\,dx - f_1 \int_0^{l_1} \left(\frac{\partial}{\partial t} + U\frac{\partial}{\partial x}\right)[M(x)v(x,t)]\,dx - P\frac{y}{s} - \int_0^{l_1} m(x)\frac{\partial^2 y}{\partial t^2}\,dx = 0, \tag{7}$$

where f_1 has the equivalent meaning for the nose tapered section that f_2 has for the tail.

The tow-rope pull is equal to the tension in the cylinder at $x = 0$, plus the form drag at the nose which we assume to be proportional to $\rho U^2 S$. Accordingly, we have $P = \frac{1}{2}c_T MU^2 L/D + \frac{1}{2}c_2 MU^2 + \frac{1}{2}c_1 MU^2$, where c_1 is the coefficient of form drag at the nose. Substituting for P and integrating (6) and (7), making use of the fact that v and y are assumed constant for $0 < x < l_1$ and for $L - l_2 < x < L$ (provided, of course, that $l_1/L \ll 1$ and $l_2/L \ll 1$), we obtain

$$\left.\begin{aligned}\left[EI\frac{\partial^3 y}{\partial x^3} + f_1 MU\left(\frac{\partial y}{\partial t} + U\frac{\partial y}{\partial x}\right) + \tfrac{1}{2}MU^2\left(c_T\frac{L}{D} + c_1 + c_2\right)\frac{y}{s}\right.\\ \left. + (m + f_1 M)x_0\frac{\partial^2 y}{\partial t^2}\right]_{x=0} = 0,\\ \left[EI\frac{\partial^3 y}{\partial x^3} + f_2 MU\left(\frac{\partial y}{\partial t} + U\frac{\partial y}{\partial x}\right) - (m + f_2 M)x_L\frac{\partial^2 y}{\partial t^2}\right]_{x=L} = 0,\end{aligned}\right\} \tag{8}$$

where

$$x_0 = \frac{1}{S}\int_0^{l_1} S(x)\,dx \quad \text{and} \quad x_L = \frac{1}{S}\int_{L-l_2}^{L} S(x)\,dx. \tag{9}$$

The other two boundary conditions required were obtained by making the reasonable assumption that there are no bending moments on the cylinder at $x = 0$ and $x = L$, or

$$\left[\frac{\partial^2 y}{\partial x^2}\right]_{x=0} = \left[\frac{\partial^2 y}{\partial x^2}\right]_{x=L} = 0. \tag{10}$$

These are similar to the boundary conditions derived by Hawthorne (1961).

3. Analysis

The problem is expressed in dimensionless terms by putting

$$\left.\begin{aligned}&\xi = \frac{x}{L}, \quad \eta = \frac{y}{L}, \quad \tau = \left[\frac{EI}{m+M}\right]^{\frac{1}{2}}\frac{t}{L^2}, \quad \beta = \frac{M}{m+M},\\ &\epsilon = \frac{L}{D}, \quad \Lambda = \frac{s}{L}, \quad \chi_1 = \frac{x_0}{L}, \quad \chi_2 = \frac{x_L}{L} \quad \text{and} \quad u = \left(\frac{M}{EI}\right)^{\frac{1}{2}}UL.\end{aligned}\right\} \tag{11}$$

Substituting into (5) we obtain

$$\frac{\partial^4\eta}{\partial\xi^4} + u^2[1 - \tfrac{1}{2}\epsilon c_T(1-\xi) - \tfrac{1}{2}c_2]\frac{\partial^2\eta}{\partial\xi^2} + 2\beta^{\frac{1}{2}}u\frac{\partial^2\eta}{\partial\xi\,\partial\tau} + \tfrac{1}{2}\epsilon(c_N + c_T)u^2\frac{\partial\eta}{\partial\xi} + \tfrac{1}{2}\epsilon c_N\beta^{\frac{1}{2}}u\frac{\partial\eta}{\partial\tau} + \frac{\partial^2\eta}{\partial\tau^2} = 0. \tag{12}$$

Similarly, the boundary conditions are

$$\left.\begin{aligned}\frac{\partial^2\eta}{\partial\xi^2} = \frac{\partial^3\eta}{\partial\xi^3} + f_1u^2\frac{\partial\eta}{\partial\xi} + \tfrac{1}{2}u^2[(\epsilon c_T + c_1 + c_2)/\Lambda]\eta + f_1\beta^{\frac{1}{2}}u\frac{\partial\eta}{\partial\tau} \\ + [1+(f_1-1)\beta]\chi_1\frac{\partial^2\eta}{\partial\tau^2} = 0 \quad \text{at} \quad \xi = 0,\end{aligned}\right\} \tag{13}$$

and at $\xi = 1$

$$\left.\frac{\partial^2\eta}{\partial\xi^2} = \frac{\partial^3\eta}{\partial\xi^3} + f_2u^2\frac{\partial\eta}{\partial\xi} + f_2\beta^{\frac{1}{2}}u\frac{\partial\eta}{\partial\tau} - [1+(f_2-1)\beta]\chi_2\frac{\partial^2\eta}{\partial\tau^2} = 0.\right\}$$

It is noted that β may in principle vary from 0 to 1; the lower limit corresponds to a very light fluid and a very heavy cylinder, and the higher limit to the opposite case. However, the assumption of null buoyancy made earlier (§2) necessitates that $\beta = \frac{1}{2}$.

Let us now consider motions of the cylinder of the form

$$\eta = Y(\xi)\, e^{i\omega\tau}, \tag{14}$$

ω being a dimensionless frequency defined by $\omega = [(M+m)/EI]^{\frac{1}{2}}\Omega L^2$, where Ω is the circular frequency of motion which in general is complex. The system will be stable or unstable accordingly as the imaginary part of ω is positive or negative.

The system under consideration has an infinite number of degrees of freedom. The complete solution of the dynamical problem therefore involves the determination of the infinite set of frequencies of the normal modes of oscillation of the system, as continuous functions of the dimensionless velocity u and the 'system parameters' β, ϵ, c_N, c_T, c_1, c_2, f_1, f_2, χ_1, χ_2.

The method of analysis is to express $Y(\xi)$ as a power series in ξ (cf. Paidoussis 1966*a*), so that

$$\eta = \left[\sum_{r=0}^{\infty} A_r\xi^r\right] e^{i\omega\tau},$$

where the A_r are generally complex. Substituting into (12) and (13) we eventually obtain a 4×4 determinant which must vanish for non-trivial solution (cf. Paidoussis 1966*a*); this provides an implicit relation between ω on the one hand, and u and the system parameters on the other. A sufficient number of terms in the power series must be used to approximate adequately the shape of the body in the course of its motions. It was found that up to 40 terms were necessary in order to determine ω to three significant figures.

4. The frequency as a function of flow velocity

For any given physical system we suppose that the system parameters can be calculated or measured, and that they are independent of the flow velocity. Using typical values of these parameters, the complex frequencies of some of the lower modes of a number of systems are calculated, for increasing values of the dimensionless flow velocity u, starting with $u = 0$. The method of computation using a digital computer is essentially as described by Paidoussis (1966*a*).

The complex frequencies of the lowest four modes of the system for some

typical cases, plotted as Argand diagrams, are shown in figures 3 to 6. We note that for $u = 0$ the cylinder is essentially a free-free beam as there is no tension on the tow-rope; accordingly, the dimensionless frequencies of the so-called

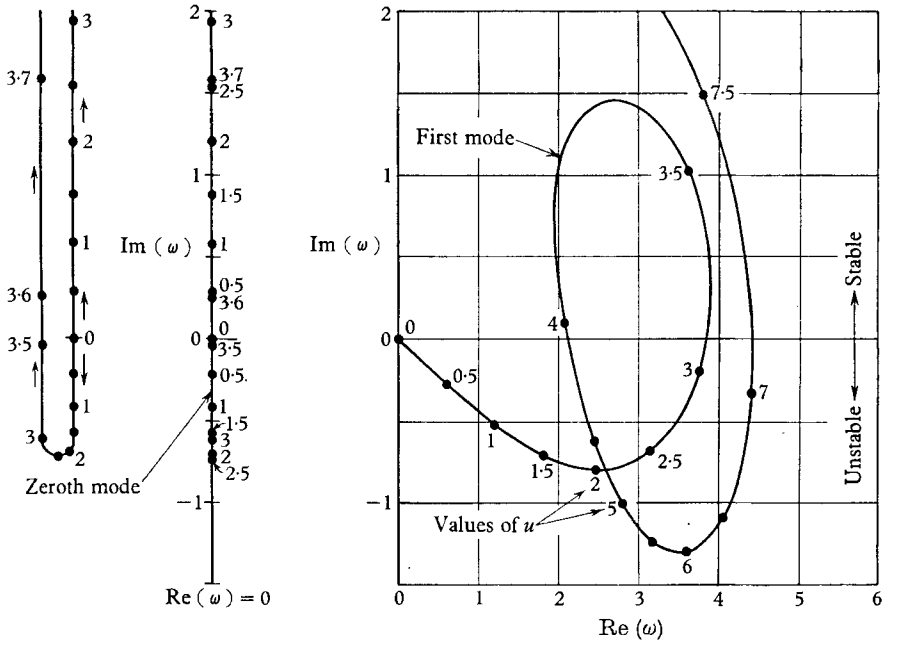

FIGURE 3. The dimensionless complex frequency of the zeroth and first modes of a system with $\epsilon c_N = \epsilon c_T = 1, f_1 = 1, c_1 = 0, f_2 = 0{\cdot}8, c_2 = 0{\cdot}2, \Lambda = 1, \chi_1 = \chi_2 = 0{\cdot}01$.

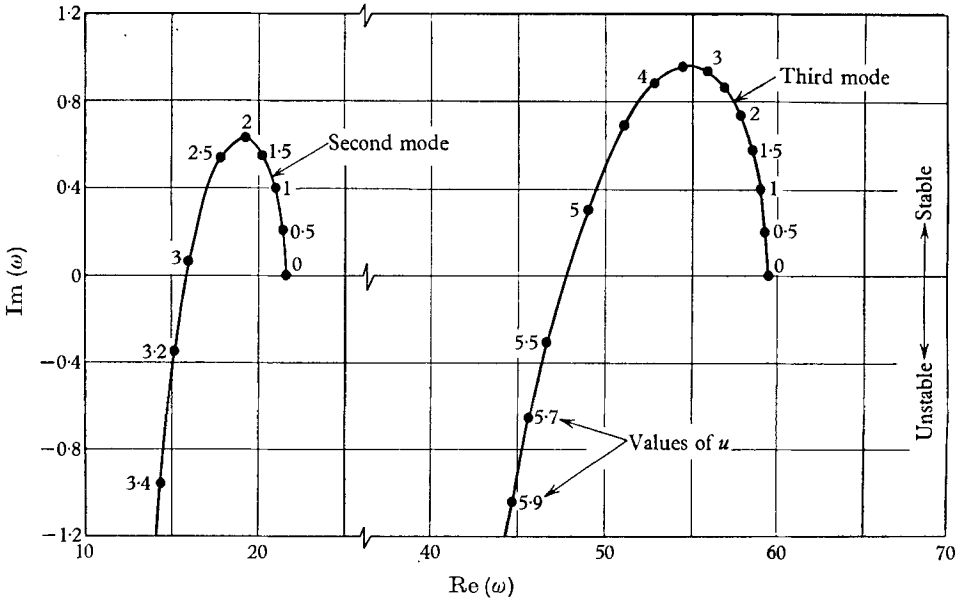

FIGURE 4. The dimensionless complex frequency of the second and third modes of a system with $\epsilon c_N = \epsilon c_T = 1, f_1 = 1, c_1 = 0, f_2 = 0{\cdot}8, c_2 = 0{\cdot}2, \Lambda = 1, \chi_1 = \chi_2 = 0{\cdot}01$.

second, third and higher modes, for $u = 0$, correspond to those of a free-free beam [cf. figures 4 and 6; minor differences between the free-free beam frequencies and those shown arise from departures from cylindrical geometry at the nose and tail of the cylinder]. The reason for calling these modes 'second', 'third', etc. is mainly for their similarity in shape (for $u = 0$) to those of a pinned-free beam, to which this system is related.

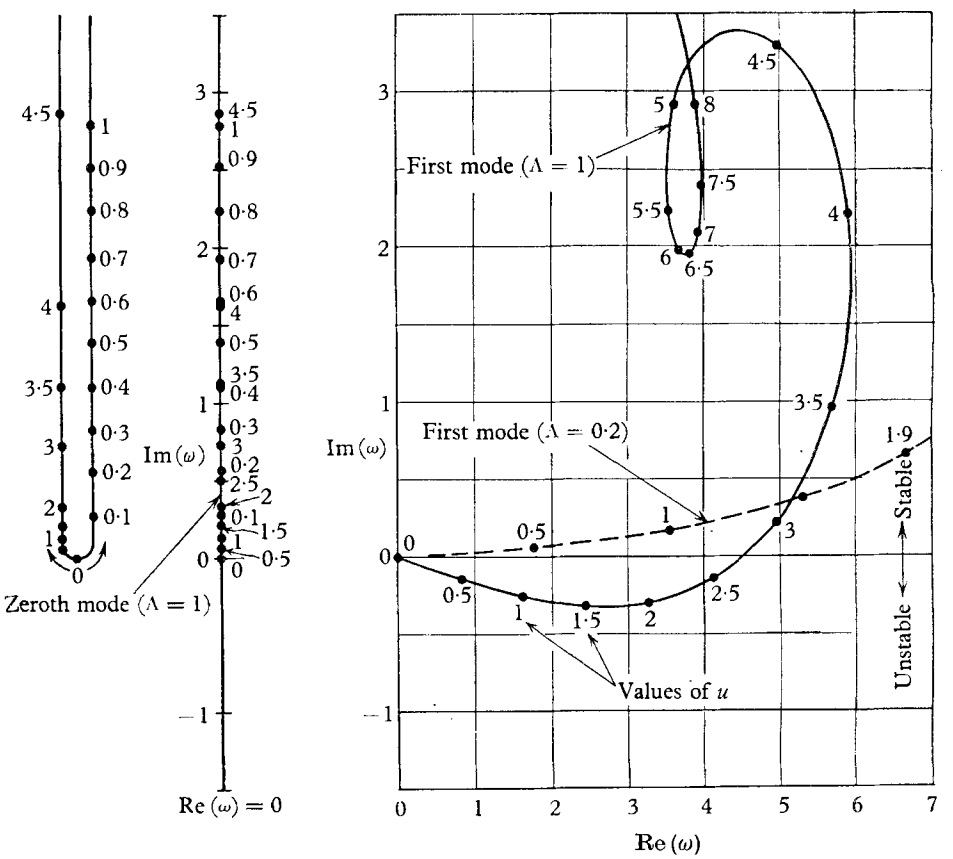

FIGURE 5. The dimensionless complex frequency of the zeroth and first modes of a system with $\epsilon c_N = \epsilon c_T = 1$, $f_1 = 1$, $c_1 = 0$, $f_2 = 0{\cdot}4$, $c_2 = 0{\cdot}6$, $\Lambda = 1$, $\chi_1 = \chi_2 = 0{\cdot}01$; also the first mode with $\Lambda = 0{\cdot}2$.

The 'zeroth' and 'first' modes (cf. figures 3 and 5) correspond to essentially rigid-body motions, at least for very low values of u. At $u = 0$, the frequency $\omega = 0$ corresponds to rigid-body rotation about the point where the tow-rope is attached to the towing vessel; for $u > 0$, however, evidently two modes emanate from this point, one oscillatory and the other non-oscillatory. The zeroth mode generally remains on the [Im(ω)]-axis and the instability associated with this mode will be called 'yawing'; this instability, according to linear theory, involves a divergent non-oscillatory deviation from the position of rest, with or without flexing.

Figures 3 and 4 show the frequencies of the lowest four modes of a cylinder

with a perfectly streamlined nose ($f_1 = 1$) and an almost perfectly streamlined tail ($f_2 = 0{\cdot}8$), such that the form drag at the nose may be considered to be essentially zero at the nose ($c_1 = 0$) and appreciable at the tail ($c_2 = 0{\cdot}2$); the tow-rope is as long as the cylinder ($\Lambda = 1$). At low flow the system is evidently unstable in the zeroth and first modes and, at higher flow velocities, in the second

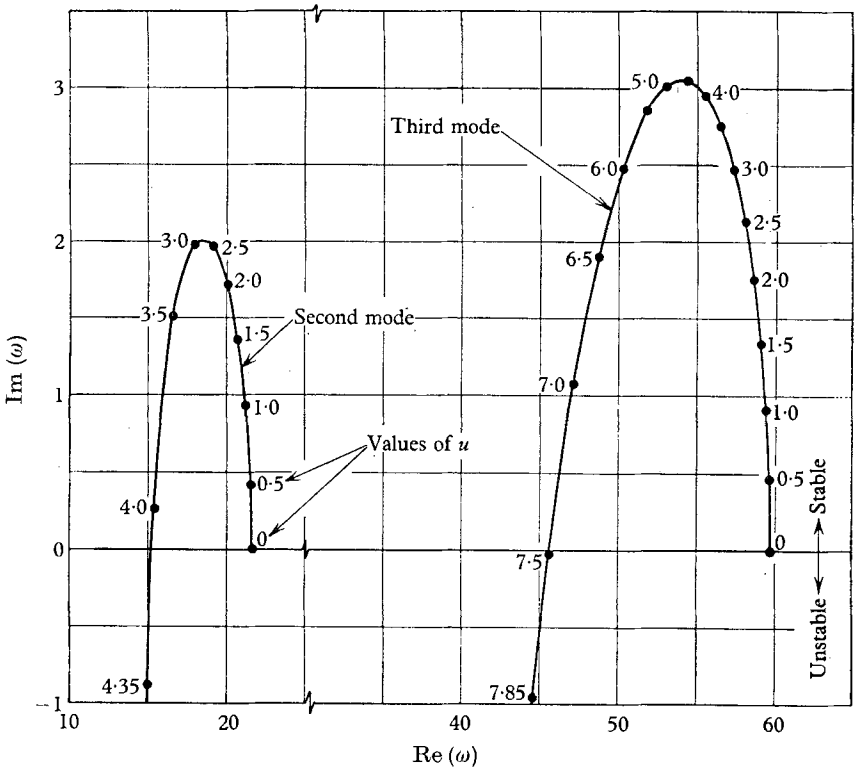

FIGURE 6. The dimensionless complex frequency of the second and third modes of a system with $\epsilon c_N = \epsilon c_T = 1, f_1 = 1, c_1 = 0, f_2 = 0{\cdot}4, c_2 = 0{\cdot}6, \Lambda = 1, \chi_1 = \chi_2 = 0{\cdot}01$.

and third modes also. The locus of a mode on the [Im(ω)]-axis always has two branches; in the case of the zeroth mode, one branch has Im(ω) > 0 for all u, whereas the other leads to instability. The behaviour of this mode is clarified by the supplementary diagram at the far left of the figure. The fact that the zeroth and first modes are unstable for arbitrarily small u indicates that the system is unstable as a rigid body, since flow-induced forces will then be very small in comparison with the flexural restoring forces; thus this is similar to the instability of a balloon moored to a mast. The second and third modes behave essentially as if the upstream end of the cylinder were pinned or clamped (Paidoussis 1966*a*). It is of particular interest that the system may be unstable in at least one of its modes for all values of u (figures 3, 4).

A comparison of figures 3 and 5 shows the effect of a blunter tail (smaller f_2 and higher c_2) on the behaviour of the zeroth and first modes of a particular system with $f_1 = 1$, $c_1 = 0$, $\epsilon c_N = \epsilon c_T = 1$, $\chi_1 = \chi_2 = 0{\cdot}01$ and $\Lambda = 1$. We see that the

blunter tail renders the system stable in its zeroth mode for all u, both branches of this mode being on the positive [Im(ω)]-axis (figure 5). Also, the locus of the first mode crosses to the stable region at a smaller value of u. Thus blunting the tail has a stabilizing effect on the system in its zeroth and first modes. Similarly, from figures 4 and 6 we see that blunting the tail has a stabilizing effect also on the second and third modes of the system.

Also shown in figure 5 is the effect of reducing the length of the tow-rope from $\Lambda = 1$ to $\Lambda = 0{\cdot}2$. We see that the first mode is stabilized quite effectively. [Values of u such that $\omega = 0$ are independent of f_1, c_1, Λ, χ_1 and χ_2. Changing Λ will change the numerical values of Im(ω) in the case of the zeroth mode, but the basic behaviour of the mode will not change. In the case of $\Lambda = 0{\cdot}2$ in figure 5, the locus of the zeroth mode cannot cross to the unstable region as it would have to pass through $\omega = 0$; since there is no solution with $\omega = 0$ and $u > 0$ for $\Lambda = 1$, there cannot be one for $\Lambda = 0{\cdot}2$.]

The effect of the various system parameters on stability will be considered further in the next section.

The results obtained here are inconsistent with those reported in appendix II of Hawthorne's (1961) paper, in which the behaviour of the system with increasing flow velocity (towing speed) was considered to be similar to that of the dynamically analogous system of a flexible tube conveying fluid (Benjamin 1961); thus the system was considered to be stable up to a critical towing speed which was assumed to be associated with a buckling form of instability. This critical towing speed was calculated by obtaining solutions to the equation of motion satisfying $\omega = 0$, without doing complex frequency calculations. One drawback of this type of analysis is the difficulty in interpreting the results; thus, having found such a point of neutral stability, it is not evident whether the system is stable or unstable above or below this point.

Now from figures 3 to 6 we see that the only solutions with $\omega = 0$ are associated with the zeroth and first modes, and do not represent thresholds of instability, except for $u = 0$. After careful study of this matter the author has come to the conclusion that the critical velocities reported by Hawthorne do indeed correspond to points of neutral stability associated with the zeroth mode (cf. $u \approx 3{\cdot}5$, figure 3), but they do not represent thresholds of instability.

5. The conditions of stability

The complex frequency calculations shown in figures 3–6 establish the existence of several types of instability. In this section the ranges of flow velocity over which the system is unstable are calculated as functions of the various system parameters, f_1, f_2, c_1, c_2, ϵc_N, etc. The results are presented as maps of stability showing the effect of the most important system parameters.

Figure 7 shows the effect on stability of the shape of the tail of a cylinder with $\epsilon c_N = \epsilon c_T = 1$, $\Lambda = 1$ and a perfectly streamlined nose ($f_1 = 1$, $c_1 = 0$). The form drag coefficient at the tail is arbitrarily taken to have a numerical value

$$c_2 = 1 - f_2,$$

on the reasonable assumption that, as the tail becomes blunter, f_2 is reduced and the form drag coefficient increases; however, $c_2 = (1-f_2)/2$ or $= (1-f_2)^2$, etc. could equally well have been chosen. The upper region marked 'first-mode oscillatory instability' corresponds to the second unstable loop of the first mode (cf. figure 3). We see that the range of u over which the system is stable is enlarged as the tail becomes blunter. For $f_2 > 0{\cdot}71$ approximately, the system is

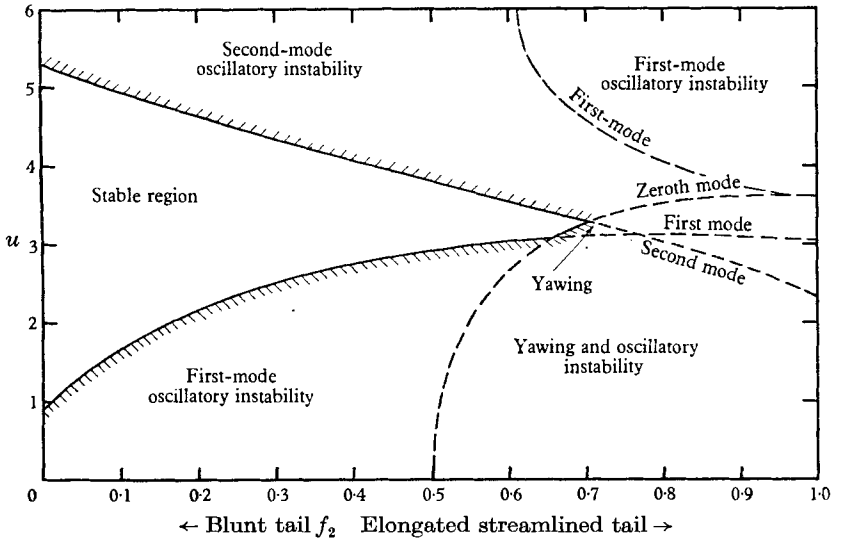

FIGURE 7. Stability map showing the effect of the tail shape for a system with $\epsilon c_N = \epsilon c_T = 1$, $f_1 = 1$, $c_1 = 0$, $\Lambda = 1$, $\chi_1 = \chi_2 = 0{\cdot}01$ and $c_2 = 1-f_2$.

unstable over the whole range of flow velocities in at least one of its modes. In such cases, where the system is unstable in more than one of its modes, it is not possible, at least at this stage, to determine the precise behaviour of the system.

Figure 8 shows the effect of the tail shape on the same system but with the length of the tow-rope reduced by half ($\Lambda = 0{\cdot}5$). In this case, the threshold for third-mode oscillatory instability is also shown. Also shown is that in some cases, namely for $f_2 < 0{\cdot}5$ approximately, the second mode regains stability at sufficiently high u. We see that the stable region is much larger in this case. For $f_2 < 0{\cdot}15$ approximately, first-mode oscillatory instability is not possible, and for $f_2 < 0{\cdot}05$, second-mode oscillatory instability does not occur either. This suggests a practical operational shape: a system with a stream-lined nose, a very blunt tail and $\Lambda = 0{\cdot}5$ can be stable over a wide range of flow velocities, namely from $u = 0$ to $u > 9$.

Figure 9 shows the effect of the tow-rope length on a system with

$$\epsilon c_N = \epsilon c_T = 1,$$

a perfectly streamlined nose and a medium-blunt tail ($f_2 = 1-c_2 = 0{\cdot}6$). We see, as would be expected from the previous two figures, that reducing the tow-rope length enlarges the stable region. For $\Lambda = 0{\cdot}15$, for instance, there appears to be a region of yawing $0 < u < 2{\cdot}65$; at higher u, the system is stable up to $u \approx 6{\cdot}2$

which is the threshold of third-mode oscillatory instability. For lower f_2, the region of yawing at low u disappears entirely, as shown in figure 10 for

$$f_2 = c_2 = 0{\cdot}5.$$

In this case the stable region, for $\Lambda < 0{\cdot}21$, extends from $u = 0$ to $u > 6{\cdot}5$. It is of particular interest that Λ has to be made quite small before it can have a

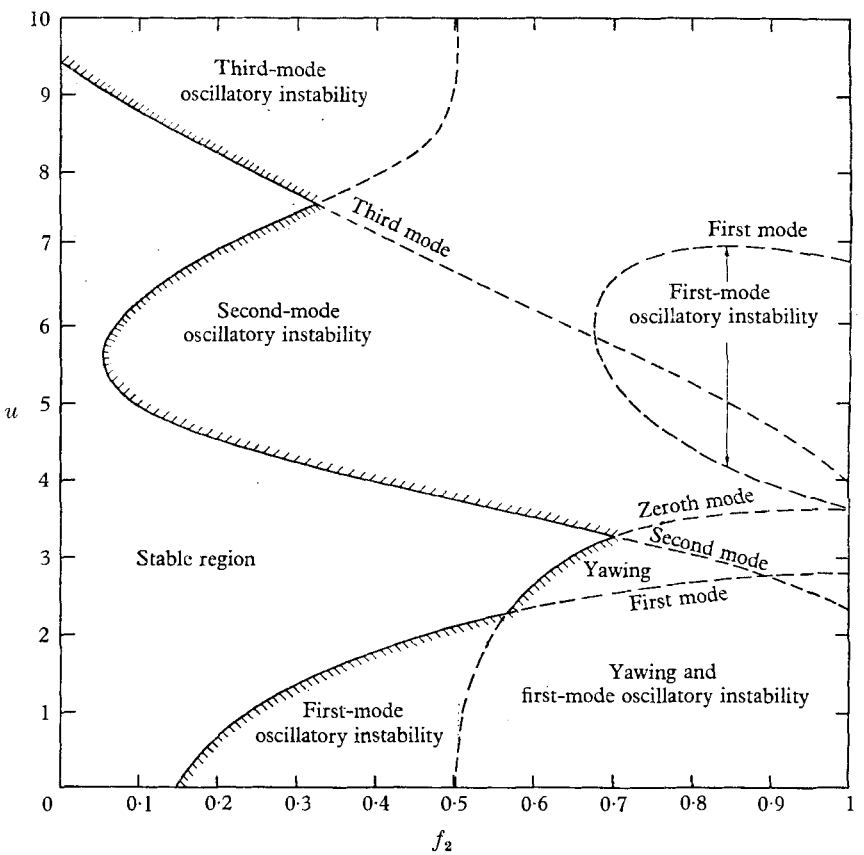

FIGURE 8. Stability map showing the effect of the tail shape for a system with $\epsilon c_N = \epsilon c_T = 1$, $f_1 = 1$, $c_1 = 0$, $\Lambda = 0{\cdot}5$, $\chi_1 = \chi_2 = 0{\cdot}01$ and $c_2 = 1 - f_2$.

significant stabilizing effect on second- and third-mode oscillatory instabilities. For even blunter tail shapes, however, effective stability extends to larger values of Λ than shown in figures 9 and 10. The combination of a blunt tail and a relatively short tow-rope can be relied upon to stabilize the system to fairly large values of u.

As was stated previously, the critical flow associated with the zeroth mode ($\omega = 0$), representing the cessation of yawing is independent of Λ, f_1 and c_1. For the particular combination of the other system parameters in figure 10 (and in figure 11), yawing instability is not possible.

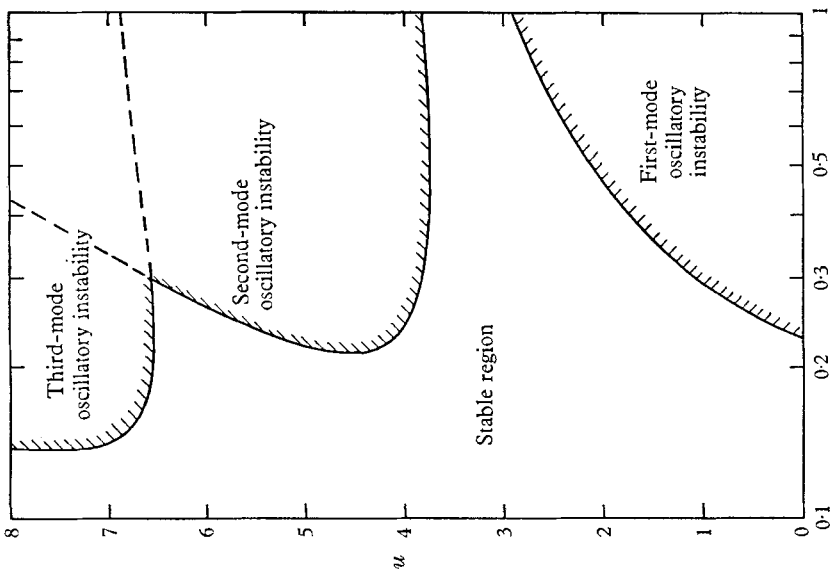

FIGURE 10. Stability map showing the effect of Λ for a system with $\epsilon c_N = \epsilon c_T = 1, f_1 = 1, c_1 = 0, f_2 = 0{\cdot}5, c_2 = 0{\cdot}5, \chi_1 = \chi_2 = 0{\cdot}01$.

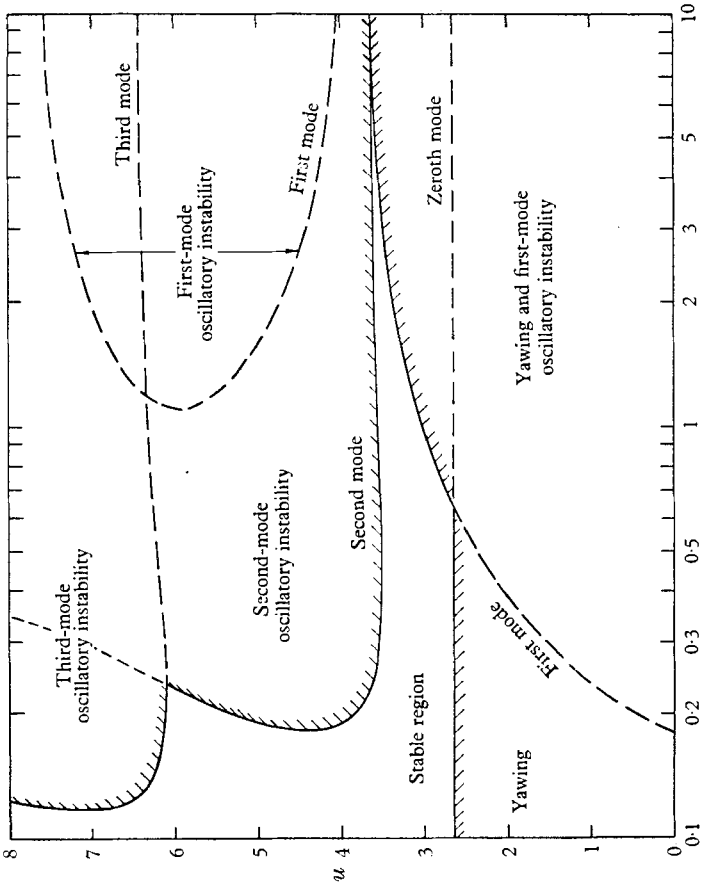

FIGURE 9. Stability map showing the effect of Λ(= ratio of tow-rope length to cylinder length) for a system with $\epsilon c_N = \epsilon c_T = 1, f_1 = 1, c_1 = 0, f_2 = 0{\cdot}6, c_2 = 0{\cdot}4, \chi_1 = \chi_2 = 0{\cdot}01$.

Figure 11 shows the effect of the shape of the nose for two systems with $f_2 = 0{\cdot}5$, $c_2 = 0{\cdot}5$, $\Lambda = 1$ and $f_2 = 0$, $c_2 = 1$, $\Lambda = 0{\cdot}5$, respectively, and

$$\epsilon c_N = \epsilon c_T = 1$$

in both cases. Here we arbitrarily set $c_1 = 1 - f_1$. We see that reducing f_1 has a marked destabilizing effect on the system. Accordingly, for optimum stability

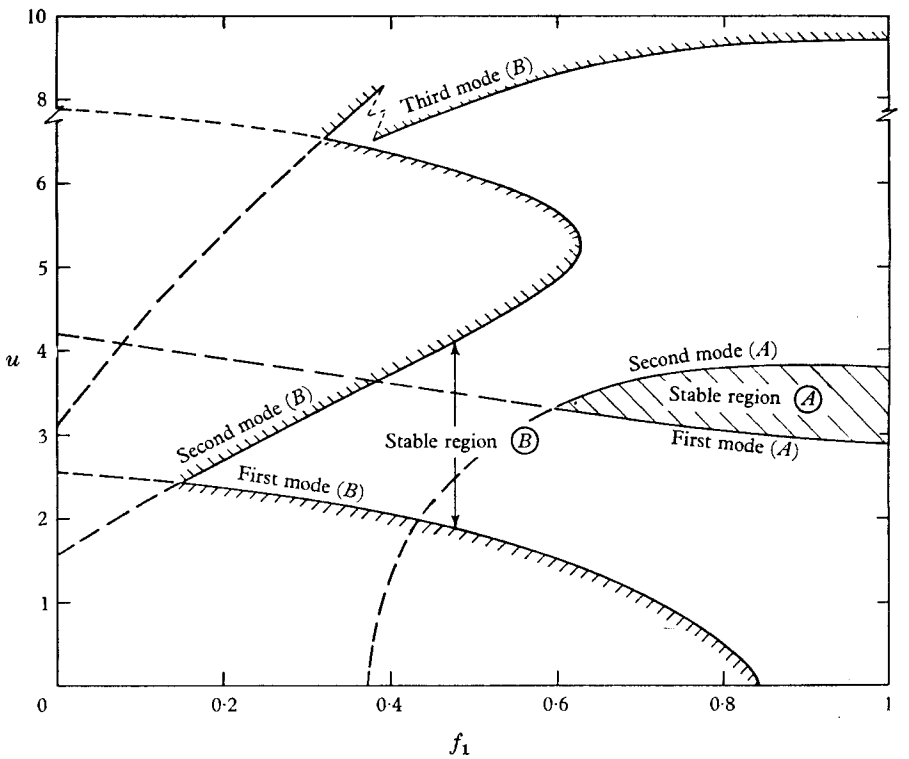

FIGURE 11. Stability map showing the effect of the nose shape for two systems with $\epsilon c_N = \epsilon c_T = 1$, $\chi_1 = \chi_2 = 0{\cdot}01$, $c_1 = 1 - f_1$. (*A*), $f_2 = 0{\cdot}5$, $c_2 = 0{\cdot}5$, $\Lambda = 1$; (*B*), $f_2 = 0$, $c_2 = 1$, $\Lambda = 0{\cdot}5$.

the nose should be made as streamlined as possible. (It should be remarked here that increasing c_1 actually has a stabilizing effect.) It is noteworthy, nevertheless, that, provided the tail is sufficiently blunt (case B), the system may be effectively stable even with a less than perfectly streamlined nose.

Figure 12 shows the effect of ϵc_N and ϵc_T on stability. Here we take $c_N = c_T$. Increasing ϵc_N and ϵc_T signifies either a more slender cylinder ($\epsilon = L/D$) or one with higher frictional coefficients. Since in practice the construction will be such that c_N and c_T be as small as possible, to avoid excessive towing drag, we shall regard figure 12 as representing the effect on stability of the slenderness of the cylinder.

We see that manipulating ϵ alone is not a very effective means of stabilizing the system. Only the zeroth mode is radically affected by varying ϵ. This can be important in some cases in conjunction with small Λ and f_2; thus in figure 9, if

$\epsilon c_N = \epsilon c_T = 1{\cdot}5$ instead of unity, the unstable region associated with the zeroth mode entirely disappears.

The parameters χ_1 and χ_2 in the above calculations were taken to be

$$\chi_1 = \chi_2 = 0{\cdot}01$$

in all cases. Although it would have been more consistent to vary χ_1 and χ_2 with changing f_1 and f_2, it is found that, provided they remain small, χ_1 and χ_2 have very little effect on the dynamics of the system.

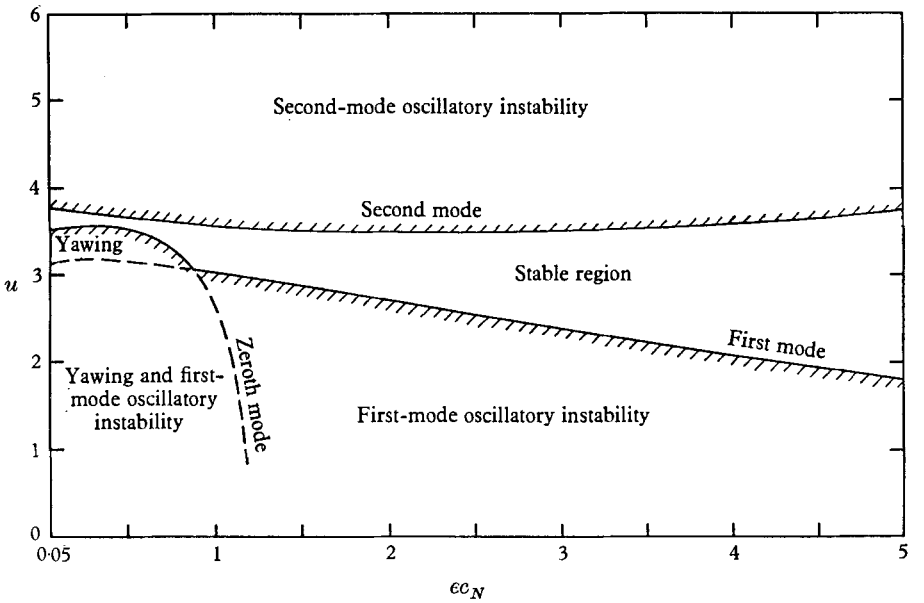

FIGURE 12. Stability map showing the effect of ϵc_N and ϵc_T for a system with $c_T = c_N$ $f_1 = 1$, $c_1 = 0$, $f_2 = 0{\cdot}6$, $c_2 = 0{\cdot}4$, $\Lambda = 1$, $\chi_1 = \chi_2 = 0{\cdot}01$.

Because there are many system parameters, it is not practicable to produce universal stability curves, as could be done for cylinders with both ends supported (Paidoussis 1966*a*) for instance. Besides, the exhaustive study of the effect of the various system parameters is both not very illuminating and quite laborious; for instance, the calculations shown in any one of the figures 7 to 12 require several hours of computer time.

From figures 7 to 12 we may conclude that for maximum stability the system must have: (*a*) a streamlined nose, (*b*) a blunt tail, (*c*) a fairly slender cylinder, and (*d*) a short tow-rope.

6. Experiments

A number of experiments were conducted with flexible cylinders held in flow by a length of string attached to their upstream end. The aim of the experiments was to test the theory discussed in the previous sections. It is stressed at the outset that these were not meant to be exhaustive experiments. Their main purpose

was (*a*) to discover whether the various types of instability predicted by theory do in fact occur, and (*b*) to provide some experimental data, particularly regarding the thresholds of the various instabilities, for quantitative comparison with theory.

Apparatus

The flexible cylinders were made by casting liquid silicon rubber ('Silastic') into specially made moulds. The cylinders were made hollow, so that they would be of neutral buoyancy when submerged in water. In fact, when submerged, the manufactured cylinders very slowly settled to the bottom; however, the measured

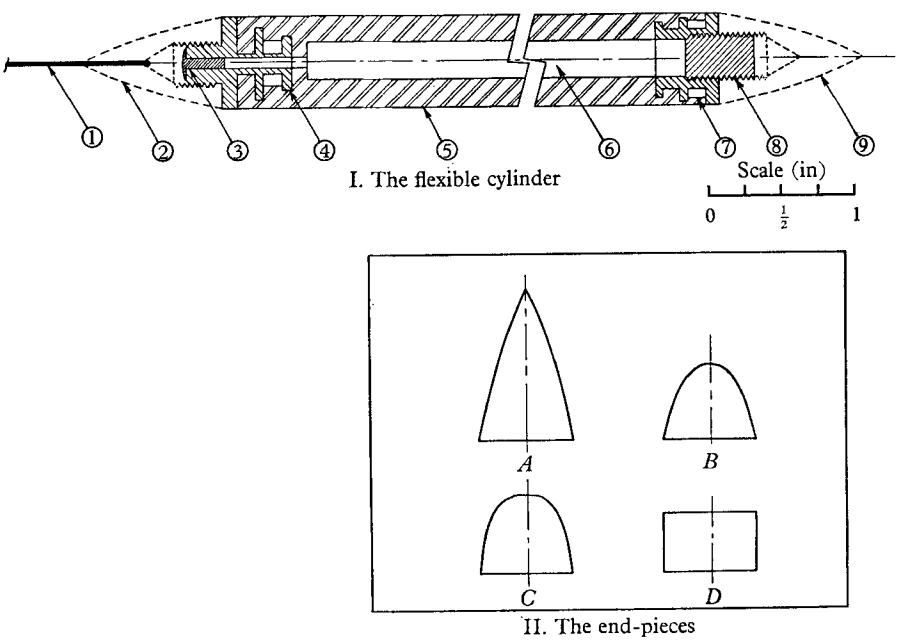

FIGURE 13. The construction of the flexible cylinders used in the experiments and the shape of the end-pieces (for cylinder I): 1, nylon thread (tow-rope); 2, perspex nose end-piece; 3, perspex plug glued to produce water-tight seal; 4, perspex adaptor for receiving end-pieces; 5, silastic rubber cylinder; 6, ¼ in. diameter hole for buoyancy; 7, perspex spacers to prevent rotation of adaptors; 8, glued threaded plug; 9, perspex tail end-piece.

specific gravity was never greater than 1·01. At its two extremities the cylinder was fitted with threaded protrusions (see figure 13) over which could be screwed tapered perspex end-pieces. Several types of tapered ends were made in order to assess their effect on stability.

Two cylinders were used: cylinder I was 13·9 in. long (without the ends), 0·68 in. diameter (EI = 1290 lb. in.^{3}/sec^2), and cylinder II was 9·8 in. long (without the ends), 0·54 in. diameter (EI = 490 lb. in.^{3}/sec^2).

The experiments were conducted in a vertical, 3 in. diameter, glass test-section. The cylinder hung in the flow. This vertical arrangement was preferred to a horizontal one, as the cylinder started out being in the centre of the flow-tube

when the flow was turned on. (In a horizontal arrangement, the slightest departure from a specific gravity of unity—even arising from changes in water temperature–forced the cylinder to the top or the bottom of the flow tube.) Gravity and buoyancy were considered to have negligible net effect on lateral motions of the cylinder. Clearly a more spacious test-section would have been preferable; nevertheless, because the flow was fully developed turbulent pipe flow over most of the flow range of interest, it is considered that wall effects did not have much effect on the onset of instability. Of course this does not necessarily hold when large oscillations have developed; thus wall effects may have affected the transition from one form of instability to another, in cases where there was no intervening return to stability (cf. general observations).

Straightening devices were placed ahead of the test-section in order to eliminate secondary-flow effects. Gauzes were placed downstream of the slender support which held the string, upstream of the cylinder, to eliminate non-uniformity in the flow introduced by the support. The length of the string could be varied.

The flow velocity was measured with an orifice. The maximum flow attainable was about 13 ft./sec. During tests the flow velocity was increased in small steps, and time was allowed at each step to observe developments, if any.

General observations

In the description of observed phenomena given below, we use observations and measurements obtained from experiments with cylinder I. In each case the behaviour of the system is given in detail for $\Lambda = \frac{1}{2}$; subsequently, deviations from this behaviour for other values of Λ are noted.

(i) *Cylinder with elongated nose A and tail A* (*see figure* 13). At very low flow velocities ($u < 0{\cdot}8$) the system was stable and the cylinder remained in its central position of rest. At higher flow velocities 'criss-crossing' oscillation developed, i.e. oscillation during which the tail moved in the opposite direction to the nose, about the position of rest, such that the two limiting positions of the cylinder formed an X; the instantaneous inclination of the string relative to the position of rest was in the opposite direction to that of the cylinder. The frequency and amplitude of oscillation increased with flow; thus at $u = 0{\cdot}8$, $\omega = 2{\cdot}1$; at $u = 2$, $\omega = 3{\cdot}2$; at $u = 2{\cdot}9$, $\omega = 4{\cdot}4$. These were low-frequency oscillations corresponding to 0·3 to 1 c/s. The amplitude increased to the point where the cylinder almost touched the flow-tube. At the lower flows, motion of the cylinder involved no perceptible flexure; at the higher flows there was appreciable flexure, with the tail 'dragging' during oscillation. These oscillations were interpreted as corresponding to first-mode oscillatory instability.

For $u > 2{\cdot}3$ the cylinder assumed a bowed ('banana') shape in the course of oscillation. At $u > 3$ the amplitude of oscillation decreased, and at $u = 3{\cdot}6$ the oscillation ceased while the cylinder retained a 'banana' shape. This is interpreted as the point where first-mode oscillatory instability ceases, but the system is still unstable in its zeroth mode (cf. figure 8, e.g. for $f_2 = 0{\cdot}8$), in a form of yawing involving flexing ('buckling').

This buckled shape was retained up to $u = 4$, where amplified second-mode

oscillations began. The motion developed in one plane, but after a few cycles of oscillation changed to a three-dimensional motion involving whirling of the cylinder. In shape the oscillations looked like amplified free vibrations of a free-free beam in its first mode (cf. §4). The frequency of oscillation was about 2·4 c/s ($\omega = 17$).

The amplitude of oscillation increased with flow up to $u \approx 5$, where the oscillation became discontinuous. It appeared as if the cylinder was oscillating in its first-mode (criss-crossing) again, with a second-mode oscillation superposed; however, the amplitude of oscillation was quite large and the cylinder frequently hit the flow-tube. This probably corresponds to the second unstable loop of the first mode (cf. figure 8). This continued up to $u = 7{\cdot}2$ where third-mode amplified oscillation developed. The frequency was about 7 c/s ($\omega = 49$). Whirling took place in this case also.

The behaviour of the system for $\Lambda = 1$ and $\Lambda = \frac{1}{4}$ was essentially as above. For $\Lambda = 1$, the amplitude of oscillation was generally much larger and hitting the flow-tube rendered observations less reliable. This was exaggerated for $\Lambda = 3$, and the observations were very difficult to interpret.

For $\Lambda = \frac{1}{8}$ the observations were considerably different. In this case criss-crossing oscillation was not observed. Instead the cylinder took a skewed configuration at $u > 1{\cdot}2$. This presumably corresponds to yawing at low u, where the fluid forces are too small to cause flexing of the cylinder. Increasing the flow gradually transformed the skewed cylinder to a banana-shaped one, as before. Evidently this corresponds to a case where, in the absence of first-mode oscillatory instability (cf. figure 9), yawing instability asserts itself even at low flow. Moreover, in this case second-mode oscillation, which started at $u = 5{\cdot}1$, was not disrupted, continuing in a regular manner up to $u = 7{\cdot}5$, where third-mode oscillation started. Just before the establishment of the regular second-mode oscillation ($\omega = 23$), an unusual, lower frequency oscillation ($\omega = 7{\cdot}7$) developed at $4{\cdot}6 < u < 5{\cdot}1$. It was not unlike second-mode oscillation in shape and it was quite regular. This is further discussed in the next section.

(ii) *Cylinder with elongated nose A and medium-blunt tail C.* In this case the cylinder was stable for $u < 1{\cdot}1$. Between $u = 1{\cdot}1$ and $1{\cdot}6$ some small amplitude criss-crossing was observed which was not as continuous as in the previous case. At higher flows, up to $u = 5{\cdot}5$, the system was stable. No yawing instability developed, which agrees qualitatively with the theoretical results of figure 8 for $f_2 < 0{\cdot}5$.

At $u = 5{\cdot}5$ second-mode amplified oscillation developed ($\omega = 16$). The motion in this case remained in one plane. At $u > 5{\cdot}9$ some whirling occurred, however. This oscillation persisted with increasing flow up to $u = 7{\cdot}4$, where discontinuous third-mode oscillation was observed. Evidently the flow was not quite high enough to produce fully developed third-mode amplified oscillation.

The qualitative behaviour of the system for $\Lambda = 1$ was essentially as above. The flow-range over which criss-crossing occurred, however, was larger

$$(1{\cdot}1 < u < 2{\cdot}5).$$

For $\Lambda = \frac{1}{4}$ no criss-crossing at all could be observed, and for $\Lambda = \frac{1}{8}$ the system

was stable over the full flow range, from $u = 0$ to 7·4. These observations are in qualitative agreement with the theoretical results of figure 10.

(iii) *Cylinder with elongated nose A and very blunt tail D.* In this case the tail end-piece was not tapered at all. The system was found to be stable over the full flow-range. This was the case for $\Lambda = \frac{1}{4}$ and $\Lambda = \frac{1}{8}$ as well. For $\Lambda = 1$, however, second-mode oscillation developed at $u = 6{\cdot}3$ and continued to maximum flow. No whirling took place. At lower flows the system was stable.

These observations are in qualitative agreement with the theoretical results for $f_2 = 0$ in figures 7 and 8; the only discrepancy is that no first-mode oscillation was observed for $\Lambda = 1$.

(iv) *Cylinder with blunt nose and elongated tail.* In one experiment the medium-blunt end-piece C was used as the nose. The tail was the same elongated end-piece as in (i). The observations displayed no essential qualitative or quantitative difference from those of (i). This would appear to contradict the theoretical prediction shown in figure 11, which could be intepreted to signify that blunting the nose destabilizes the system. On reflexion, however, perhaps theory and experiment do not disagree after all. In this connexion, two points must be made. First, theory actually predicts that *reducing* f_1 destabilizes the system. Since reduction of f_1 or f_2 from unity comes about mainly by flow-separation, we can see that, whereas an end-piece used as the tail may have a low value of f_2, the same end-piece used as the nose does not necessarily have a low value of f_1. Secondly, increasing the nose form-drag coefficient c_1 actually stabilizes the system. (The results in figure 11 were obtained on the assumption that c_1 and f_1 are related by $c_1 = 1 - f_1$.)

(v) *Cylinder with elongated nose and elongated, finned tail.* The cylinder in this case was the same as in (i), except that the tail had a rectangular fin in one diametral plane. The fin was of the same width as the cylinder diameter and extended over the full length of the tail. The dynamic behaviour of the cylinder in this case was essentially as if the fin were not there, at least up to the point of inception of second-mode oscillation. Oscillation tended to be in the plane of the fin. In the case of second- and third-mode instabilities, oscillation would develop in the plane of the fin; then, a slight rotation of the plane of motion disrupted oscillation. Accordingly second- and third-mode oscillation was discontinuous.

In a subsequent experiment, a second fin was placed on the tail at 90° to the first. Once again this proved to be an unsatisfactory way of stabilizing the system. Essentially the only difference to the case without fins was that second-mode amplified oscillation occurred at slightly higher flow velocities, i.e. at $u = 4{\cdot}5$. The oscillation was continuous and no whirling took place.

(vi) *Cylinder with ring stabilizer.* In this case a rubber ring, 0·785 in. diameter, was fitted concentrically over the cylinder just ahead of the tail end-piece (cylinder diameter = 0·68 in.). The nose and tail were as in (i). The effect on stability was notable. There was no criss-crossing oscillation, nor yawing, the system remaining stable up to $u = 3{\cdot}7$. For $u > 3{\cdot}7$ there were small amplitude, damped, second-mode oscillations which increased in amplitude and continuity with flow. At $u > 4{\cdot}4$ the oscillations were essentially continuous, but the amplitude did not exceed $\frac{1}{2}$ in. It was difficult to decide whether the system was un-

stable or not, because of the relatively small amplitude of motion. Similarly, with third-mode instability; third-mode, small amplitude, continuous oscillations developed at $u = 6{\cdot}4$ and persisted to maximum flow.

Thus, although the ring had a definite stabilizing effect, it was not nearly as effective as the very blunt end D, as described in (iii).

Quantitative comparison with theory

Direct quantitative comparison is not possible since this requires knowledge of the numerical values of the system parameters c_N, c_T, f_1, f_2, c_1 and c_2, which are unfortunately not known. Consequently, for purposes of comparison, experimental values of thresholds of instability, etc., were compared with more than one set of the corresponding calculated values. Thus, the experimental results for the cylinder with the elongated tail A were compared with calculated values for $f_2 = 1$, $c_2 = 0$ and for $f_2 = 0{\cdot}7$, $c_2 = 0{\cdot}3$. The choice of the latter set is not entirely arbitrary, drawing on previous experience from experiments with clamped-free cylinders (Paidoussis 1966*b*). Similarly, the medium-blunt end C was compared with $f_2 = c_2 = 0{\cdot}5$ and $f_2 = 0{\cdot}3$, $c_2 = 0{\cdot}7$. In all cases presented below, c_2 was taken to be numerically equal to $1 - f_2$, and $f_1 = 1 - c_1 = 1$. Concerning c_N and c_T, they were taken to be $c_N = c_T \sim 0{\cdot}05$ (cf. Paidoussis 1966*b*), so that

$$\epsilon c_N = \epsilon c_T = 1.$$

In the experimental calculations of u and ω, the flow velocity U was calculated from the volumetric flow measurement assuming a uniform velocity distribution in the test section and taking account of the cross-sectional area occupied by the cylinder. The length L was taken to be the overall length of the cylinder, including the end-pieces.

Some of the experimental results obtained are compared with theory in tables 1 to 3.

Table 1 shows the effect of shape of the tail on stability for $\Lambda = \frac{1}{2}$ in the case of cylinder I. We see that comparing tail A with $f_2 = 0{\cdot}7$, tail B with $f_2 = 0{\cdot}5$, tail C with either $f_2 = 0{\cdot}5$ or $0{\cdot}3$, and tail D with $f_2 = 0$, the theoretical model predicts the behaviour of the system reasonably well. In numerical terms, agreement is also reasonably good, except for the fact that the experimental thresholds for second- and third-mode instabilities are considerably higher than predicted by theory. The corresponding frequencies, surprisingly, are remarkably close.

Table 2 compares with theory the experiments with cylinder I fitted with elongated nose and tail, for various tow-rope lengths. Here again the theoretical values for $f_2 = 0{\cdot}7$ predict all essential features of the experimental observations. One remarkable occurrence is connected with the low-frequency oscillation observed between $u = 4{\cdot}6$ and $5{\cdot}1$ for $\Lambda = \frac{1}{8}$; we see that this may well correspond to the first-mode unstable loop predicted by theory to occur between $u = 5{\cdot}4$ and $7{\cdot}3$.

Table 3 similarly deals with cylinder I fitted with an elongated nose and a medium-blunt tail. We see that comparison with theory for $f_2 = 0{\cdot}5$, or better for $f_2 = 0{\cdot}3$, gives quite reasonable agreement with experiment.

The experimental results obtained with cylinder II were essentially the same as those with cylinder I.

Description		Theor. $f_2 = 1$	Exp. tail A	Theor. $f_2 = 0{\cdot}7$	Exp. tail B	Theor. $f_2 = 0{\cdot}5$	Exp. tail C	Theor. $f_2 = 0{\cdot}3$	Exp. tail D	Theor. $f_2 = 0$
Criss-crossing oscillation (first-mode osc. instability)	u	0–2·8	0·8–3·6	0–2·5	0·8–1·6	0–2·1	1·1–1·6	0–1·4	—	—
	ω	0–4·1	2–7	0–4·8	1·9–2·3	0–4·5	~3·2	0–3·2	—	—
Stationary yawing instability (zeroth mode instability without first- or second-mode oscillation	u	—*	3·6–4·0	2·5–3·3	—	—	—	—	—	—
Stable region	u	—	—	—	1·6–4·8	2·1–3·7	1·6–5·5	1·4–4·2	0–7·4†	0–9·4
Second-mode oscillation threshold (second-mode osc. instability)	u	2·3	4·0	3·3	4·8	3·7	5·5	4·2	—	—
	ω	18	17	16	16	16	15	18	—	—
Second-mode with superposed first-mode oscillation (concurrence of first- and second-mode osc. instabilities)	u	3·6–6·8	5–7·2	5·3–6·6	—	—	—	—	—	—
Third-mode oscillation threshold (third-mode osc. instability)	u	4·0	7·2	5·8	7·1	6·7	7·4‡	7·6	—†	9·4
	ω	52	49	48	48	48		48		53

* Signifies that the phenomenon described does not occur.

† Maximum flow available corresponds to $u = 7{\cdot}4$.

‡ Third-mode oscillation not fully developed.

TABLE 1. The effect of tail shape on stability (cylinder I; nose A; $\Lambda = \frac{1}{2}$)

Description		$\Lambda = 1$			$\Lambda = \frac{1}{2}$			$\Lambda = \frac{1}{4}$			$\Lambda = \frac{1}{8}$		
		Theor. $f_2 = 1$	Exp.	Theor. $f_2 = 0{\cdot}7$	Theor. $f_2 = 1$	Exp.	Theor. $f_2 = 0{\cdot}7$	Theor. $f_2 = 1$	Exp.	Theor. $f_2 = 0{\cdot}7$	Theor. $f_2 = 1$	Exp.	Theor. $f_2 = 0{\cdot}7$
Criss-crossing oscillation (first-mode osc. instability)	u	0–3·0	0·8–3·3	0–3·1	0–2·8	0·8–3·6	0–2·5	0–2·3	0·8–3·6	0–1·5	0–0·95	—*	—
	ω	0–3·0	2–4	0–4·2	0–4·1	2–7	0–4·8	0–4·9	2–5	0–4·0	0–3·2	—	—
Stationary yawing (zeroth-mode instability alone)	u	—	3·3–3·8	3·1–3·3	—	3·6–4·0	2·5–3·3	2·3–2·4	3·6–4·2	1·5–3·3	0·95–3·6	1·2–3·7	0–3·3
Second-mode oscillation threshold (second-mode osc. instability)	u	2·3	3·8	3·3	2·3	4·0	3·3	2·4	4·2	3·4	2·6	5·1	—
	ω	18	17	15·5	18	17	16	18	18	18	20	23	—
Second-mode with superposed first-mode oscillation (concurrence of first- and second-mode osc. instabilities)	u	3·6–7·0	4·4–6·8	4·6–6·9	3·6–6·8	5·0–7·2	5·3–6·6	3·8–6·3	5·0–7·2	5·8–6·7	—	4·6–5·1†	5·4–7·3‡
Third-mode oscillation threshold (third-mode osc. instability)	u	4·0	7·0	5·8	4·0	7·2	5·8	4·1	7·2	5·7	4·0	7·5	5·8
	ω	52		47	52	49	48	52	49–56	50	53	49–56	53

* Signifies that the phenomenon described does not occur.

‡ First-mode oscillation alone; $\omega = 7{\cdot}0$–$8{\cdot}2$.

† Regular low-frequency oscillation, in shape like second-mode, preceding higher frequency second-mode oscillation, $\omega = 7{\cdot}7$.

TABLE 2. The effect of tow-rope length on stability (cylinder I; nose A; tail A)

Description		$\Lambda = 1$ Theor. $f_2 = 0{\cdot}5$	$\Lambda = 1$ Exp.	$\Lambda = 1$ Theor. $f_2 = 0{\cdot}3$	$\Lambda = \frac{1}{2}$ Theor. $f_2 = 0{\cdot}5$	$\Lambda = \frac{1}{2}$ Exp.	$\Lambda = \frac{1}{2}$ Theor. $f_2 = 0{\cdot}3$	$\Lambda = \frac{1}{4}$ Theor. $f_2 = 0{\cdot}5$	$\Lambda = \frac{1}{4}$ Exp.	$\Lambda = \frac{1}{4}$ Theor. $f_2 = 0{\cdot}3$	$\Lambda = \frac{1}{8}$ Theor. $f_2 = 0{\cdot}5$	$\Lambda = \frac{1}{8}$ Exp.	$\Lambda = \frac{1}{8}$ Theor. $f_2 = 0{\cdot}3$
Criss-crossing oscillation	u	0–2·9	1·1–2·5	0–2·5	0–2·1	1·1–1·6	0–1·4	0–0·5	—*	—	—	—	—
(first-mode osc. instability)	ω	0–4·6	2–3	0–4·3	0–4·5	~3·2	0–3·1	0–1·5	—	—	—	—	—
Stationary yawing instability (zeroth-mode instability alone)	u	—	—	—	—	—	—	—	—	—	—	—	—
Stable region	u	2·9–3·8	2·5–5·2	2·5–4·4	2·1–3·7	1·6–5·5	1·4–4·2	0·5–4·0	0–5·9	0–4·5	0 – > 8	0–7·4†	0 – > 8
Second-mode oscillation	u	3·8	5·2	4·4	3·7	5·5	4·2	4·0	5·9	4·5	—	—	—
threshold (second-mode osc. instability)	ω	15·2	13	15·4	16·6	15	17·5	19·5	17	21·9	—	—	—
Third-mode oscillation	u	6·9	7·4‡	8·1	6·7	7·4‡	7·7	6·5	—†	7·5	—	—	—
threshold (third-mode osc. instability)	ω	46		46	48		48	51	—	53	—	—	—

* Signifies that the phenomenon described does not occur.

† Maximum flow available corresponds to $u = 7{\cdot}4$.

‡ Third-mode oscillation not fully developed.

TABLE 3. The effect of tow-rope length on stability (cylinder I; nose A; tail C)

7. Conclusion

The experiments, conducted with apparatus of the simplest kind, demonstrated a number of phenomena, most of which have apparently not been observed hitherto. The experiments appeared to confirm the essential features of the dynamical problem as predicted by theory. In a sense, the existence of flexural instabilities is the most important finding of this work. As we have seen, the cylinder may be stable as a rigid body, yet for sufficiently high towing speeds it may be unstable in one of its flexural modes. Apart from purely theoretical considerations, this is of practical importance also.

Quantitative agreement between experiment and theory cannot be assessed definitively, until a means is found for determining the values of c_N, c_T, c_1, c_2 and particularly f_1 and f_2. Nevertheless, even on the basis of present knowledge, it is possible to make intelligent estimates of these parameters, mainly based on experience from previous experiments (Paidoussis 1966*b*). On that basis, quantitative agreement between experiment and theory is seen to be fair, as demonstrated in tables 1 to 3, although clearly it leaves a good deal to be desired.

In discussing agreement between experiment and theory, it is recalled that, in the theoretical model, motions are assumed to occur in one plane. The question arises of how applicable this is in a case, such as in the experiments, where the cylinder is equally free to move in any plane; would the additional freedom significantly affect the stability conditions? The answer is that it would not, because motions in any two mutually perpendicular planes, according to linearized theory, are independent of each other; hence the most general motion of the system is equivalent to the superposition of two mutually independent motions, each subject to identical stability considerations. In practice it may be expected that unstable motion may start in a plane of greatest weakness. Once unstable motion develops, however, non-linear forces come into play and the motion may be expected to be three-dimensional in general, as it was indeed found to be in most experiments.

The above of course do not apply in situations where the system jumps from instability A to instability B without an intervening return to stability; in such cases it would be unreasonable to expect the experimental threshold for instability B to agree closely with the theoretical one, since the latter is always evaluated on the assumption that prior to the inception of instability the system is stable and at its position of rest. In fact, there is no *a priori* reason to expect instabilities beyond the first one to materialize at all; according to linear theory, just beyond the threshold of the first instability the amplitude of motion should increase without limit. Evidently, in this case, the non-linear forces which come into play after the onset of instability have a limiting effect on amplitude.

It should also be mentioned that the present theory does not take account of damping forces, other than those associated with the flow; this may partly explain why the thresholds of instability are virtually always higher than predicted.

Of course, a great deal of work remains to be done, particularly on the experimental side. However, even with the present study, it is possible to make a

number of recommendations regarding optimum stability of the system. The two main ones are the following: the tail must be as blunt as possible, and the tow-rope as short as possible. The experiments do not show any advantage in making the nose particularly well streamlined, which does not entirely agree with theory. In practice, of course, the desire to minimize drag would dictate a well streamlined nose in any case. It should also be borne in mind that in practice the tow-rope cannot be made very short, without running the risk of compound instabilities involving both the towing vessel and the towed cylinder, particularly when the former is small.

In terms of application of this work, it was shown that, provided that the tail is blunt, a system may be designed which would be stable to high towing speeds. Fins, according to this study, are not an effective stabilizer; however, fins of much greater surface area may be more successful. Ring stabilizers at the tail are more effective, but apparently not as good as a blunt tail; in this case also, however, a ring stabilizer different than the one used might well be more effective.

This work was conducted while the author was employed in the Reactor Research Division of Atomic Energy of Canada Ltd. at Chalk River, Ontario. The author is grateful to Mr R. I. Hodge and Atomic Energy of Canada for allowing him to conduct this investigation which has no direct nuclear application. The author is also grateful to Professor W. R. Hawthorne of Cambridge for his interest and encouragement in the course of this work.

The successful performance of the experiments owes a great deal to the provision of straight rubber cylinders—commercial tubing is entirely unsuitable. The author is grateful to Messrs F. L. Sharp and A. Celli for developing and perfecting the necessary manufacturing techniques and for assistance with the experiments.

REFERENCES

Benjamin, T. Brooke 1961 *Proc. Roy. Soc.* A **261**, 457.
Hawthorne, W. R. 1961 *Proc. Instn Mech. Engrs.* **175**, 52.
Lighthill, M. J. 1960 *J. Fluid Mech.* **9**, 305.
Munk, M. M. 1924 *NACA Rept.* no. 184.
Paidoussis, M. P. 1966*a* *J. Fluid Mech.* **26**, 717.
Paidoussis, M. P. 1966*b* *J. Fluid Mech.* **26**, 737.
Taylor, G. I. 1952 *Proc. Roy. Soc.* A **214**, 158.